

This article was downloaded by: [Tomsk State University of Control Systems and Radio]

On: 21 February 2013, At: 11:59

Publisher: Taylor & Francis

Informa Ltd Registered in England and Wales Registered Number: 1072954

Registered office: Mortimer House, 37-41 Mortimer Street, London W1T 3JH, UK



Molecular Crystals and Liquid Crystals

Publication details, including instructions for authors and subscription information:

<http://www.tandfonline.com/loi/gmcl16>

Lyotropic Cholesteric and Nematic Phases of Disodium Cromoglycate in Magnetic Fields

Heewon Lee^a & M. M. Labes^a

^a Department of Chemistry, Temple University, Philadelphia, Penna, 19122

Version of record first published: 14 Oct 2011.

To cite this article: Heewon Lee & M. M. Labes (1982): Lyotropic Cholesteric and Nematic Phases of Disodium Cromoglycate in Magnetic Fields, *Molecular Crystals and Liquid Crystals*, 84:1, 137-157

To link to this article: <http://dx.doi.org/10.1080/00268948208072137>

PLEASE SCROLL DOWN FOR ARTICLE

Full terms and conditions of use: <http://www.tandfonline.com/page/terms-and-conditions>

This article may be used for research, teaching, and private study purposes. Any substantial or systematic reproduction, redistribution, reselling, loan, sub-licensing, systematic supply, or distribution in any form to anyone is expressly forbidden.

The publisher does not give any warranty express or implied or make any representation that the contents will be complete or accurate or up to date. The accuracy of any instructions, formulae, and drug doses should be independently verified with primary sources. The publisher shall not be liable for any loss, actions, claims, proceedings, demand, or costs or damages

whatsoever or howsoever caused arising directly or indirectly in connection with or arising out of the use of this material.

Lyotropic Cholesteric and Nematic Phases of Disodium Cromoglycate in Magnetic Fields

HEEWON LEE and M. M. LABES

Department of Chemistry, Temple University, Philadelphia, Penna. 19122

(Received November 2, 1981)

Disodium cromoglycate in water (~10–15% by weight) forms a nematic liquid crystalline phase of negative diamagnetic anisotropy which readily orients in a magnetic field. The phase transition temperatures are very sensitive to the nature and concentration of the cationic species. Addition of chiral guest molecules, and in particular of amino acids, causes the phase to become cholesteric with the helix axis aligning parallel to a magnetic field. Well aligned textures of both phases are studied and a rich array of defect structures of hydrodynamic origin are observed. The pitch of the cholesteric phase can be shortened so that iridescent colors are seen at room temperature.

I INTRODUCTION

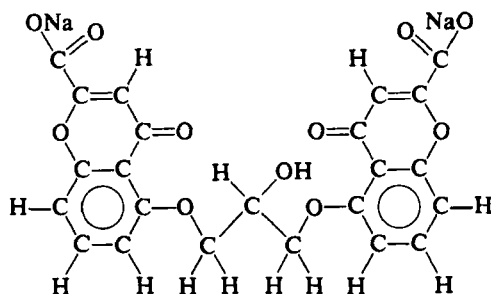
Based on either their ability to orient in a magnetic field or on their classical optical textures, certain lyotropic liquid crystals have been classified as nematics. If one defines a director \hat{n}_a for the long axis of the aggregates constituting such phases, and an associated magnetic susceptibility anisotropy $\Delta\chi_a$, they have been further classified as a "Type I" nematic lyotropic when $\Delta\chi_a > 0$, in which case \hat{n}_a would orient parallel to an applied magnetic field H , and "Type II" when $\Delta\chi_a < 0$ and \hat{n}_a is perpendicular to H .¹⁻⁴ These definitions help diagnose the phenomenological behavior of a sample without defining the structural aspects of the material. It is the issue of what is the basic structural element of lyotropic nematics that is most interesting. This element is clearly some type of aggregate of organic molecules carrying water molecules along with them, which then further adopts a superstructure. The superstructure alignment in a magnetic field induces characteristic textures which gives some clue as to its nature. This large scale aggregation appears to reach the scale of μm in dimensions. Therefore, in performing optical studies on thin samples, one may encounter the problem of structures and boundary considerations exerting influences of the same order of magnitude.

Further classification and nomenclature has recently been introduced by Yu and Saupe⁵ who studied the system sodium decyl sulfate (NaDS)-decanol-water, first reported by Lawson and Flautt.⁶ This system shows *two* nematic phases, and a direct thermally induced transition can be observed. Yu and Saupe call Type I the N_e phase (high temperature in the NaDS system) which appears to consist of rod-like micelles. The low temperature phase, Type II is referred to as the N_L phase, and is thought to consist of disc-like micelles. Both phases can be converted to a cholesteric phase by doping with chiral additives, referred to as Ch_L and Ch_c respectively.

The Ch_L phase aligns with a magnetic field so that the helix axis is \parallel to the field, whereas the Ch_c phase should undergo a Freederickz transition; that is, since the cylinder axis defined by the director \hat{n}_a prefers to be parallel to H , and the helix axis h is perpendicular to H , the helix may unwind at a sufficiently strong field.

A cholesteric Type II, Ch_L , phase has recently been reported by Acimis and Reeves⁷ who synthesized α -alanine hydrochloride decyl ester. They prepared both Ch_L and N_L phases by using the enantiomers or racemate of the ester mixed with sodium sulfate and water, a typical composition being 51% ester, 5.1% sodium sulfate in water.

A relatively simple lyotropic nematic system was reported in 1973 by Hartshorne and Woodard.⁸ It consists of a solution of disodium cromoglycate-(I) (DSCG) in water. Approximately 10% by weight of DSCG in water at room temperature, a very non-viscous solution, showed characteristic nematic optical textures, and based on an x-ray diffraction study of the " M " phase formed at higher concentrations of DSCG in water, a structural model was proposed. The M phase was suggested to consist of cylinders of diameter ~ 16 Å containing DSCG and associated water separated by varying amounts of water. In the N phase, these cylinders are so far apart that they only retain parallelism but no translational ordering. Lydon⁹ has recently modified this picture to suggest that hollow square columns of DSCG are formed defined by four molecules linked by electrostatic salt bridges. Further discussion of this model has also appeared.¹⁰



In the hope that the two components in this nematic system would make its structure and phase diagram easier to understand, we undertook a study of

this phase and the cholesteric phase which can be produced from it by adding chiral dopants. In particular, interactions of this system with a magnetic field had never been studied. Because of its low viscosity and relatively low concentration of organic in water, it seemed likely to us that short pitch chiral lyotropics could be produced by choice of appropriate dopants.

DSCG molecules, being aromatic, might be expected to align with their aromatic planes parallel to H , so that the hollow square columns pictured by Lydon⁹ would then be expected to orient \perp to H . In this sense, DSCG would be expected to be a Type II phase consisting of cylinder-like rather than disc-like micelles. Radley and Saupe¹¹ had speculated that such a phase might exist. Diehl and Tracey¹² had already reported that a diamagnetically positive (Type I) disc-like phase can exist. DSCG lyotropics therefore appear to complete the conceivable array of combinations of $\Delta\chi_a$ and shape factors.

II EXPERIMENTAL SECTION

DSCG was kindly furnished by Fisons Ltd. as a crystalline solid. It contains some tightly bound water, estimated at from 5–6 molecules in the relative humidity range 30–70%. This compound is indexed as 4H-1-benzopyran-2-carboxylic acid, 5,5'-[(2-hydroxy-1,3-propanediyl)bis(oxy)]-bis[4-oxo]-disodium salt, Registry No. 15826-37-6. Optically active additives were obtained from Aldrich or Sigma Chemical Cos. and used without further purification.

DSCG, water, and/or optically active additives were mixed in rubber septum-capped vials. For optical microscopy studies, these solutions were introduced by syringe into rectangular capillaries varying in thickness from 20 to 300 μm and of widths 4 to 10 times their thickness (Vitro Dynamics, Inc., N.J.). The ends of the capillaries were sealed with a rapid setting epoxy resin, which also served to affix the capillary to a conventional microscope slide. Differential calorimetric studies to confirm the phase relationship were performed on a Perkin-Elmer DSC-2C in sealed aluminum pans. Melting point studies were done using a Mettler FP5/52 Hot Stage between crossed polarizers on a Nikon or Zeiss microscope.

Magnetic field effects were studied by placing the capillaries on microscope slides in a 6" electromagnet for a prescribed period of time in either the x (length), y (width) or z (thickness) direction with respect to the field. Microscopic observations are then made usually between crossed polarizers to identify textural aspects.

III NEMATIC PHASE OF DSCG-ION AND $-\text{pH}$ EFFECTS

Since we intended to study the effects of chiral additives on DSCG, we first examined how ionic strength, change of counter-ion and pH affected the sys-

tem. The general features of the phase diagram presented by Hartshorne and Woodard⁸ are correct: typically one observes on heating the crystal to nematic (*N*) transition, followed by a *N* + isotropic (*I*) mixed phase, followed by a *N* + *I* to *I* transition. Table I presents data on this latter transition as a function of NaCl concentration and pH change together with the observed enthalpies.

Although pH has little effect on either the enthalpy or transition temperature, the dramatic effect of ionic strength led us to examine addition of various alkali cationic species. These data are presented in Figure 1. For each cation, a decrease in transition temperature is first observed, followed by an increase of more than 20° up to the saturation limit. Each cation shows a minimum transition at a different concentration (10^{-3} *N* for Na⁺, 10^{-4} *N* for K⁺ and 10^{-5} *N* for Li⁺). The transition temperature for the crystal → *N* transition did not show these minima, but simply decreased with concentration.

Since the *N* phase appears to consist of widely separated DSCG columnar aggregates, it is not surprising that the ionic environment would be important in determining the phase stability. Radley, Reeves and Tracey² studied the effects of counter-ion on NaDS-decanol-water phases and reported that changing the nature of the cation could induce a transition from disc-like (Type I) to cylinder-like (Type II) aggregate. Excess counter-ions might be viewed as being bound at the hydrophilic periphery of these cylindrical aggregates. The

TABLE I
Effect of NaCl and pH on the transition temperature (*N* + *I* → *I*) and enthalpy of 13% DSCG in water^a

	Added NaCl M	pH	ΔH cal g ⁻¹	Transition Temperature °K
1	—	6.9	.39	314.9
2	—	6.7	.31	313.8
3	—	6.5	.49	314.4
4	—	6.2	.29	314.7
5	—	6.0	.40	313.2
6	—	5.7	.41	314.7
7	—	5.2	.43	315.7
8	—	5.0	.36	313.7
9	—	4.7	.36	307.0
10	10 ⁻⁶	—	.40	310.2
11	10 ⁻⁵	—	.54	309.9
12	10 ⁻⁴	—	.58	310.0
13	10 ⁻³	—	.54	307.4
14	10 ⁻²	—	.40	309.9
15	10 ⁻¹	—	.49	314.7
16	0.5	—	.55	323.0
17	1	—	.43	330.5
18	1.5	—	.62	334.9

^a In these data, deionized water was employed. The transition temperatures are consistently a few degrees higher than the corresponding temperatures in triply distilled water utilized in the data presented in Figure 1.

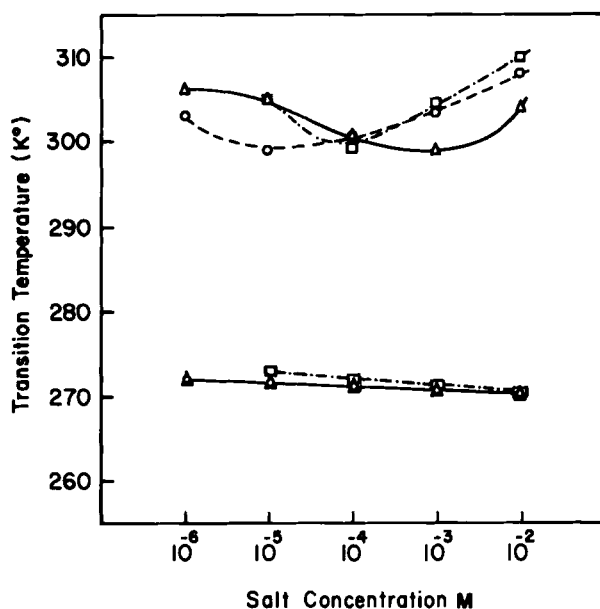


FIGURE 1 Salt effects on the transition temperatures of 13 wt % DSCG/Water (triply distilled). Upper curves: $N + I$ transition. Δ , Na^+ ; \square , K^+ ; \circ , Li^+ . Lower curves: $C \rightarrow N$ transition.

reason for the variable minima in the ionic effects, and the non-systematic, small, enthalpic changes are difficult to explain without considerable structural knowledge.

IV. NEMATIC PHASE OF DSCG-MAGNETIC FIELD EFFECTS

The N phase of DSCG shows a tendency to spontaneously form a plane texture in the glass capillaries. Between two glass plates treated by rubbing the interior glass walls (scrubbing with a piece of paper), that tendency is most profound. Table II shows the effect of a 19 kG magnetic field on $\sim 1\text{ }\mu\text{m}$ thick samples treated in various ways. The degeneracy of the plane texture is broken when a

TABLE II

Effect of 19 kG magnetic field on 13 wt % DSCG-water at 21°C between glass plates:
—, unaligned texture; Δ, plane texture; O, homogeneous texture.

Glass Treatment	Time(hr)								
	1	2	3	4	5	6	7	11	24
alcoholic KOH	—	—	—	Δ	Δ	Δ	Δ	Δ	Δ
chromic acid	—	—	—	Δ	Δ	Δ	Δ	Δ	Δ
rubbing	Δ	Δ	Δ	O	O	O	O	O	O

magnetic field is applied in *either* the x or y direction and a homogeneous texture with the long cylindrical axis being perpendicular to the field is achieved. Even when a magnetic field is applied in the z direction, the homogeneous director is not perturbed. This is to be expected for a cylindrical rod oriented \perp to H with $\Delta\chi < 0$. Figure 2 depicts these effects.

During the application of the field, characteristic defect patterns develop which are illustrated in Figure 3 and Figure 4. When a field is applied in the y direction, an interesting pattern which looks like bamboo sticks is seen (Figure 3). Initially the distance between lines (Figure 3a) were $\sim 70\ \mu\text{m}$ and the length of the small sticks were $\sim 130\ \mu\text{m}$ or a small multiple thereof. At slightly higher fields, the lines become much longer. These defect lines decay relatively rapidly (Figures 3b–3f) in about 40 minutes, and eventually a homogeneous texture with few defects remain.

Figure 4 shows another kind of defect, a “loop” which develops when an 18 kG magnetic field is applied along the x direction. At a field of 13 kG such defect patterns do not develop even after 24 hours in the field. However, small bright spots near the edge of the capillary separated by $\sim 70\ \mu\text{m}$ are observed.

Similar superstructures have been observed in Type I nematics by Charvolin and Hendrikz¹³ (loops), Yu and Saupe⁵ (lines), and Charvolin, Levelut and Samulski¹⁴ (lines). The loop in Type I develops when a high field (20 kG) is applied in the plane (along the director), whereas the line develops when a

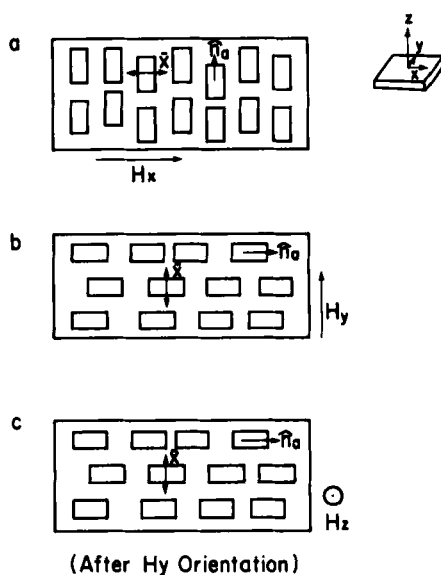
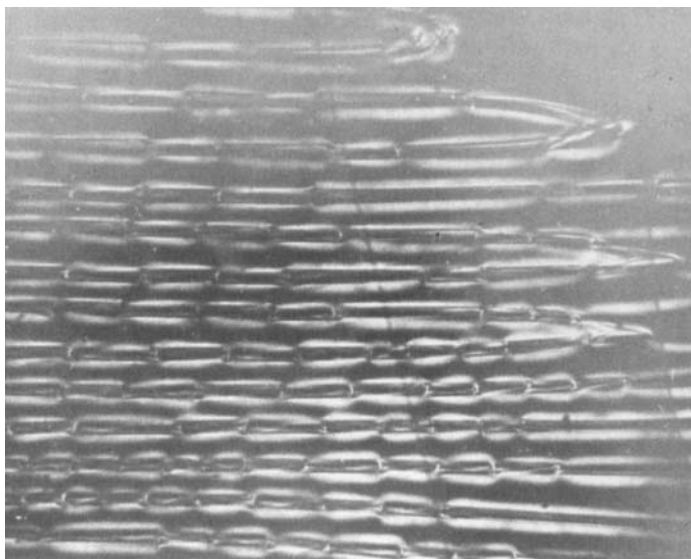
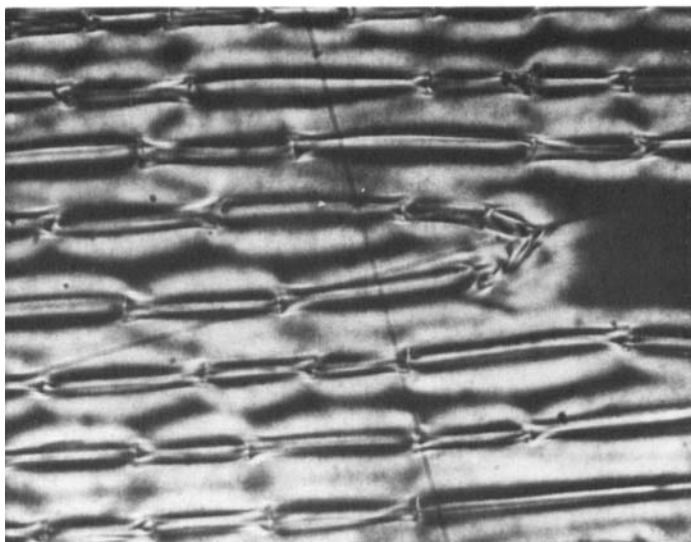


FIGURE 2 Expected position of DSCG aggregate of negative diamagnetic anisotropy in magnetic field.

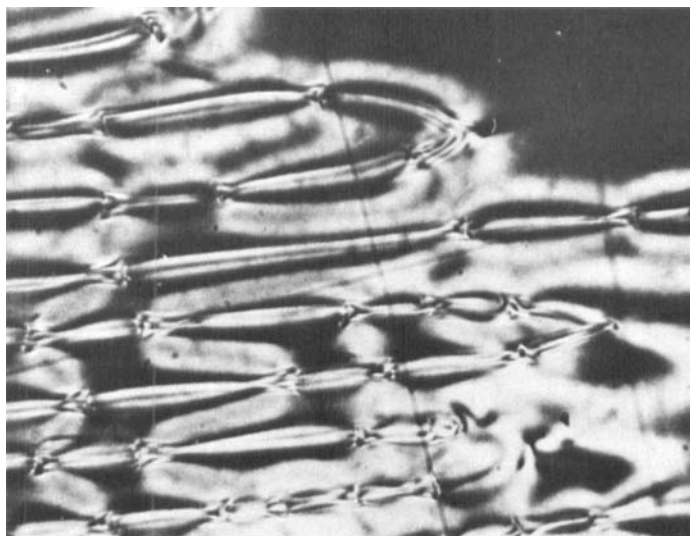


(a)

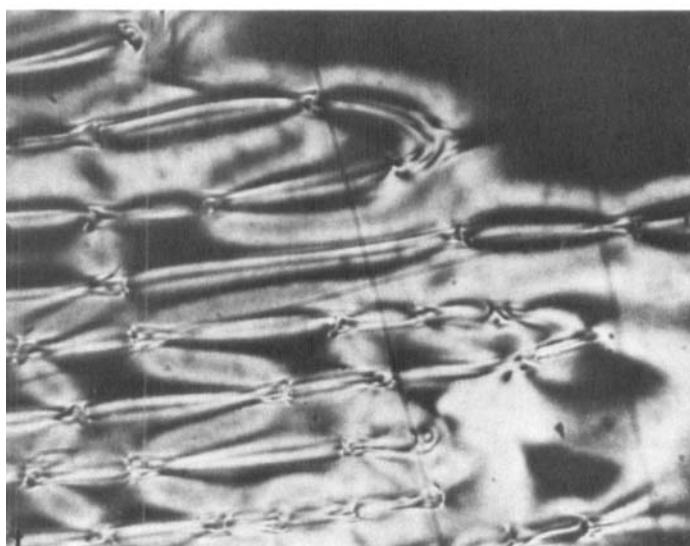


(b)

FIGURE 3 See caption after 3(f).

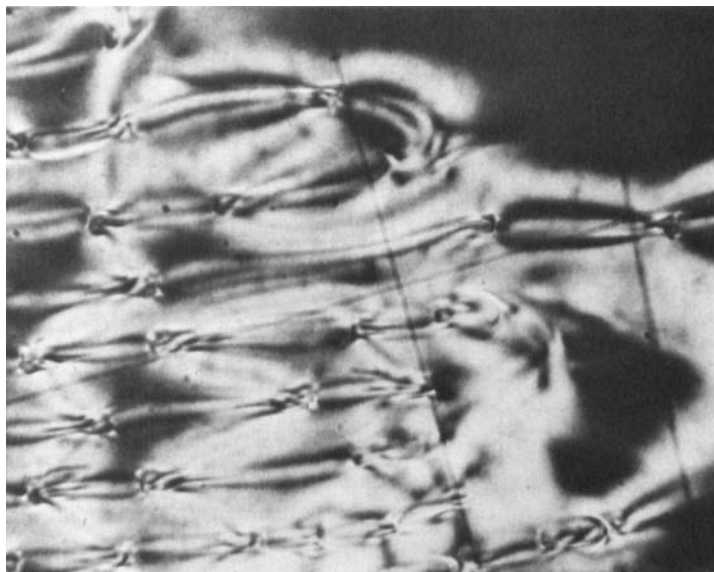


(c)

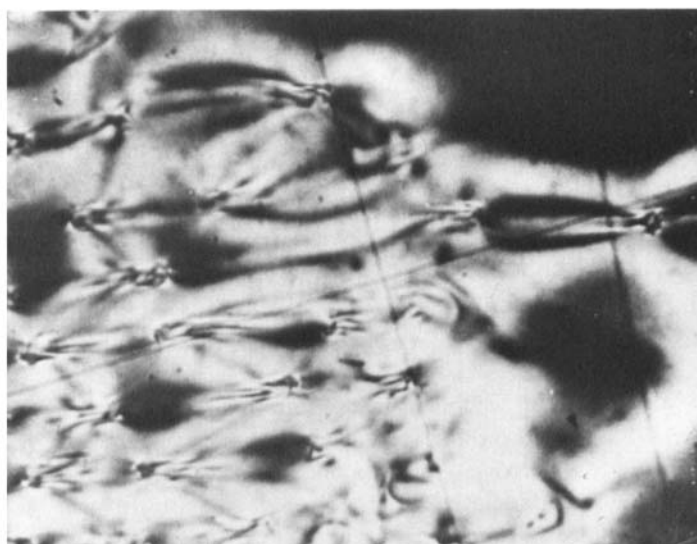


(d)

FIGURE 3 See caption after 3(f).



(c)



(f)

FIGURE 3 Characteristic defect patterns developed in a magnetic field. Sample: 17% DSCG/H₂O in a 0.1 mm thick capillary. Field: 17 kG for 18 hours at room temperature, applied horizontally. (a) immediately after removing from field, magnification $\times 125$; (b) after 10 minutes, magnification $\times 200$; (c) 20 minutes, $\times 200$; (d) 25 minutes, $\times 200$; (e) 30 minutes, $\times 200$; (f) 40 minutes, $\times 200$.

magnetic field is applied normal to the plane (\perp to the director). The explanation of such structures is that they represent borders where the nematic axes have turned in opposite direction under the action of the field. In a loop, therefore, the inside and the outside directors are out of phase. They are obviously of hydrodynamic origin and therefore depend on field strength, viscosity, and initial alignment.

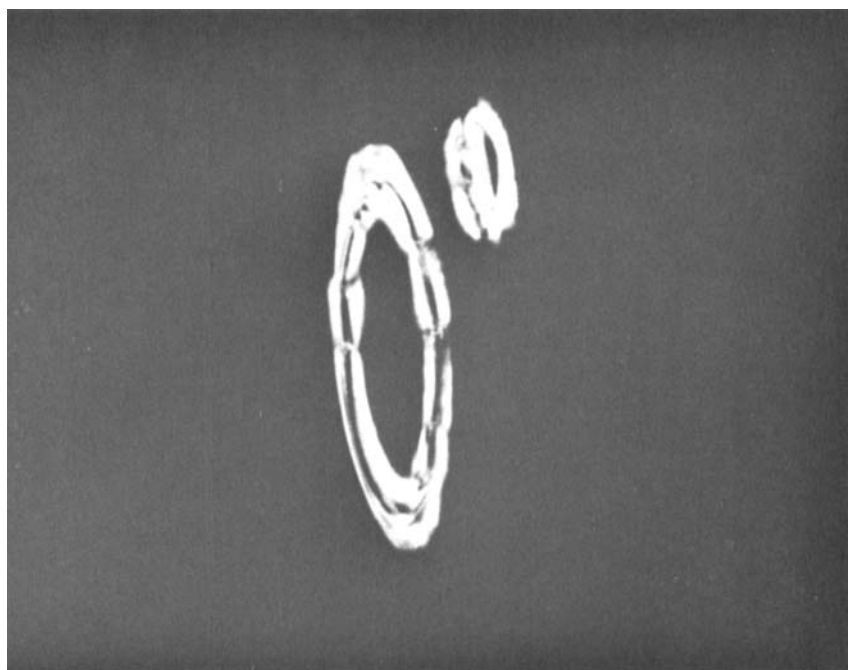
V INDUCED CHOLESTERIC PHASES OF DSCG—NATURE OF DOPANT

Cholesteric phases of DSCG can be prepared easily by adding a wide variety of water soluble chiral species. The phases still retain their relatively low viscosity and can be oriented in a magnetic field to give either the plane texture or focal conic ("fingerprint") texture, in direct analogy to thermotropic cholesteric phases of negative $\Delta\chi$. Pitch and handedness of the helical array can both be controlled by the appropriate choices of concentration and dopant. Examples of systems with pitch varying from the visible to the infrared region of the spectrum are given in this paper. A more extensive evaluation of the "helical twisting power" (HTP) of chiral molecules and their temperature dependence is underway and will appear later.

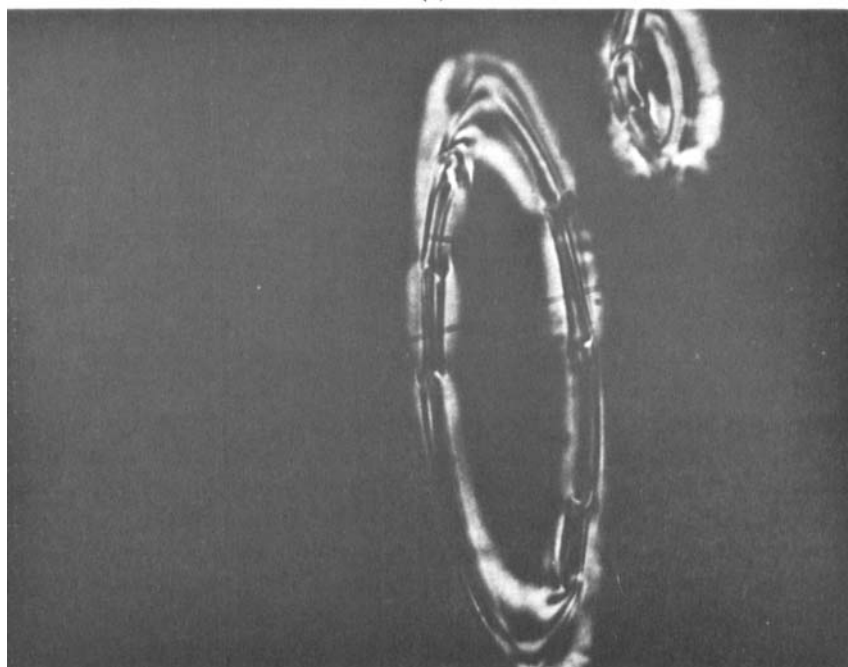
Table III is a list of chiral additives which have been screened in this work. The criteria for selection involve: water solubility, ability to hydrogen bond to carboxylic acids and/or alcohols, and/or ability to form a chiral cation. At least two effects are envisaged as being involved in making DSCG aggregates chiral: incorporation of chiral molecules as solutes in the aggregate core, and ion pairing of chiral cations with the DSCG dianion. Whether additional chiral molecules exist in the water continuum between aggregates is not as yet known.

The ratio of chiral additive to DSCG can be varied over very broad limits with profound effects on transition temperature and the resultant pitch of the helicoidal array. In particular, amino acids can be added in very large quantities to produce a cholesteric phase. Examples of the pitch-concentration relationship are given in Figures 5 and 6 for l-alanine and l-proline added to DSCG/H₂O. The pitch was measured by aligning the doped samples in a magnetic field with $H \parallel$ to the glass walls to give the "fingerprint" texture of cholesterics. Between crossed polars, one observes a series of alternately bright and dark lines associated with the precession of the director axis from a \perp to \parallel orientation with respect to the walls. The details of the magnetic orientation behavior of chiral DSCG solutions will be discussed in Section VI.

l-Alanine and l-proline both form right-handed cholesteric phases (whereas the d-enantiomers form left-handed helices). Alanine addition increases the phase transition temperature $N + I \rightarrow I$, whereas proline addition decreases the transition temperature (for example DSCG 14.8 wt % + l-alanine 10.8 wt %;



(a)



(b)

FIGURE 4 Characteristic defect patterns developed in a magnetic field. Sample: 17% DSCG/H₂O in a 0.1 mm thick capillary. Field: 18 kG for 18 hours at room temperature, applied along x direction. (a) magnification $\times 125$; (b) magnification $\times 200$.

TABLE III
Chiral dopants for DSCG/H₂O

Compound ^a	Concentration Range ^b (% by weight)	Effect ^c
Na-malate	1-15	+
Na-tartrate	1-20	-
Na-mandelate	1-20	++
Na-2-octylsulfate	1-5	+
Na-2-methylpentanoate	1-20	++
Na-2-menthoxyacetate	1-15	+
D-Glucose	1-36	++
L-(+)-Arabinose	1-36	++
D-(+)-Galactose	1-30	++
D-(+)-Mannose	1-32	++
Lactose	1-25	+
Proline	1-25	++
trans-4-hydroxyproline	1-25	++
Alanine	1-12	++
Phenylalanine	1-3	++
Lysine · HCl	1-17	++
Histidine · HCl	(d)	+
Aspartic acid	(d)	+
Serine	(d)	+

^a In most cases, only one enantiomer of the compound in question was examined (usually -l).

^b In 13-16% DSCG/H₂O.

^c ++ = very effective (high helical twisting power); + = effective; - = ineffective.

^d Solubility limited, caused phase separation in higher concentration ranges.

+31.6°C; DSCG 27.5 wt % + l-proline 14.5 wt %; -12.5°C). The helical twisting power, HTP (the proportionality constant, at low concentration between $1/P$ and C , i.e. $1/P = [\text{HTP}]C^{15,16}$) is larger for alanine than for proline at a given concentration of DSCG and temperature. The data in Figures 5 and 6 show typical concentrations of alanine and proline capable of producing pitch values between 15 and 100 μm . Above 150 μm , it is impossible to stabilize the fingerprint texture of these phases. A saturated solution of l-alanine in 13.6% DSCG gives a pitch of 9 μm at 21°C.

Short pitch with a single chiral additive has thus far been achieved only in the case of doping with trans-4-hydroxy-l-proline. However, short pitch has been achieved by suitable admixture of chiral additives in many cases. Table IV gives some examples of mixtures with pitch < 9 μm . The fingerprints become very small and difficult to measure below this region, and the characteristic iridescent colors of thermotropic cholesterics appear. Even for pitch values in the near infrared, one can see visible coloration at oblique angles to

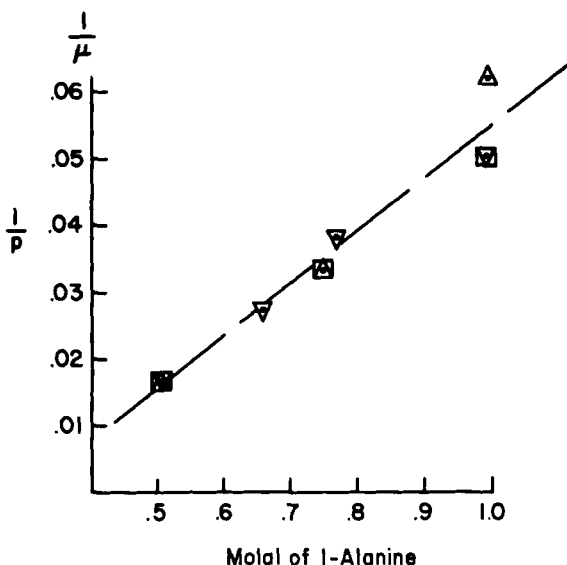


FIGURE 5 Reciprocal pitch vs Molal concentration of l-alanine. Total concentration kept constant at 0.99 Molal by adding the appropriate amount of dl-alanine. All data at 20°C. ∇ = 13%; \square = 14%; \triangle = 16% DSCG/H₂O.

the normal in both focal conic (fingerprint) and plane texture. On cooling from the isotropic phase, the plane texture appears and the typical blue \rightarrow red color sequence, i.e. pitch increasing with decreasing temperature, is seen. In the samples in Table IV, stabilization of a large monodomain region of plane texture without a magnetic field is impossible at cooling rates of 0.2°/minute (Mettler FP5/52 Hot Stage), and spherulite regimes are always seen. Further work on achieving low viscosity short pitch systems is underway.

VI CHOLESTERIC PHASE OF DSCG—MAGNETIC FIELD EFFECTS

It is well known in isotropic fluids that at some characteristic critical mechanical stress, there is a change from laminar to turbulent flow. In thermotropic nematic fluids, a periodic domain superstructure can be established by the application of magnetic (or electric) field. For example, a convective "roll pattern" can be established in a planar nematic film by applying a magnetic field perpendicular to the plates confining the sample.¹⁷ The pattern represents the coupling between flow and the distortion of director, and the dynamics depend on the viscosity of the fluid and the strength of the applied field.

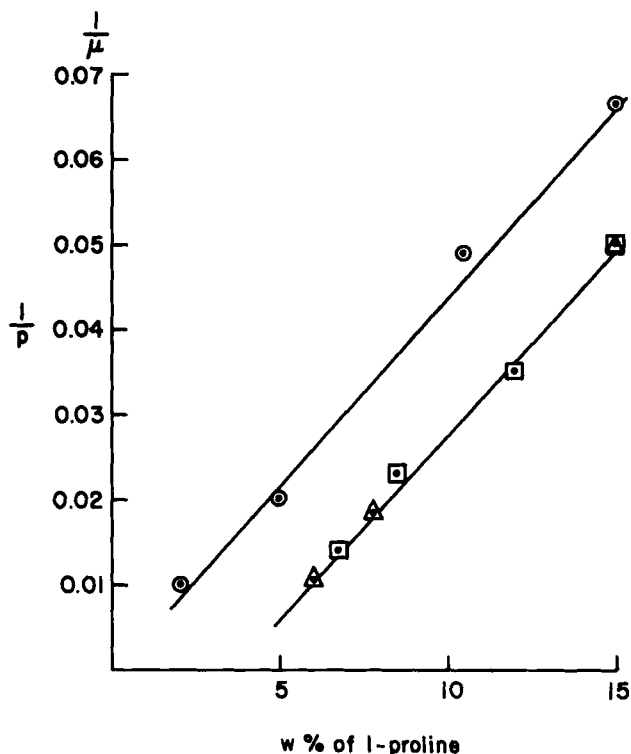


FIGURE 6 Reciprocal pitch vs concentration (wt %) of l-proline in: O, 8.3% DSCG/H₂O at 20°C; □, 16.7% DSCG/H₂O at 20°C; Δ, 13% DSCG/H₂O at 20°C.

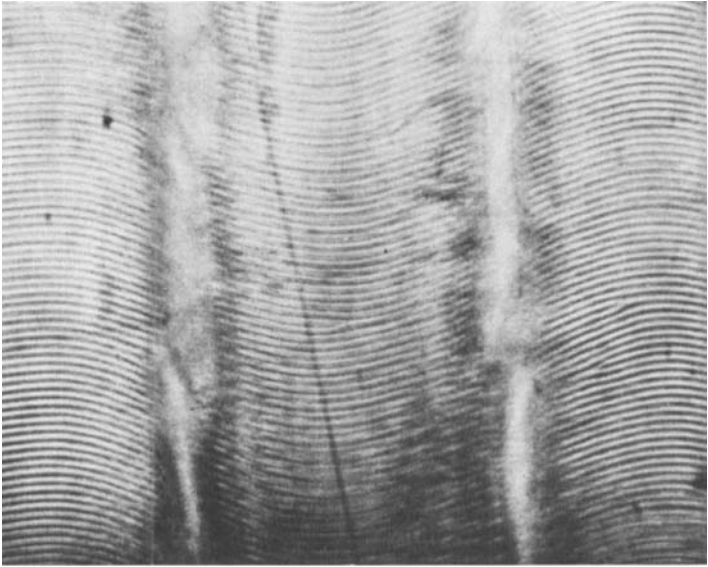
Recent results in lyotropic nematics which are magnetically oriented show similar roll patterns. Charvolin and Hendriks¹⁸ report domains created by applying $H \perp \hat{n}$ of a planar sample of Type I ($\Delta\chi > 0$) NaDS-decanol-water system. The domains can be seen in the xy plane with the roll lines $\parallel x$. In a field of 15 kG, the distance between rolls is $\sim 70 \mu\text{m}$, and decreases with increasing field. Although such roll patterns are not seen in nematic DSCG/H₂O, the cholesteric phases of DSCG have the appropriate viscoelastic coefficients to allow their easy visualization. The pitch must be less than $30 \mu\text{m}$, although this may be purely a viscosity effect, while the thickness must be $> 50 \mu\text{m}$. Application of H along the y direction induced the appearance in the xy plane of a periodic pattern shown in Figure 7a. When the field direction is changed to the x direction, the roll pattern reorients so that the flow lines are now in the y direction (Figure 7b). Note that the curvature direction of the fingerprints alternates in a regular pattern. The flow pattern pictured in Figure 7c is suggested as the explanation for the curvature of the fingerprint.

TABLE IV

Short pitch chiral lyotropic liquid crystals

Sample % in water	Helix Sense	Pitch ^a μ at 21°C	Colors on Cooling (Crossed Polarizers)
15.4% DSCG	Right	6-7	32.8° → 27.5°
9.8% l-alanine			Blue → Red
4.8% l-lysine · HCl			
15.8% DSCG	Left	3-4	34.6° → 25°
9.5% d-alanine			Blue → Red
5.1% l-lysine · HCl			
15.1% DSCG	Right	<3	30.1° → 25.0°
9.5% l-alanine			Blue → Yellow
9.5% d-lysine · HCl			
15.4% DSCG	Right	<3	27.0 → 25.0°
9.3% l-alanine			Blue → Yellow
10.8% d-lysine · HCl			
10.0% l-proline			
17.5% DSCG	Right	4	36.8° → 25°
17.3% l-proline			Blue → Yellow
6.2% l-alanine			
6.2% Na-l-mandelate			
17.5% DSCG	Right	6	34.3° → 23.5°
17.3% l-proline			Blue → Yellow
6.2% l-alanine			
1% Na-l-mandelate			
19.1% DSCG	Right	10	38.5° → 30.5°
18.9% l-proline			Blue → Red
6.8% l-alanine			
16% DSCG	Left	7.5	30.6° → 20°
8% l-lysine · HCl			Blue → Red
14% dl-alanine			
16% DSCG	Left	4	31.4° → 20°
8% l-lysine · HCl			Blue → Red
14% d-alanine			
16% DSCG	Right	4	31.4° → 20°
8% l-lysine · HCl			Blue → Red
14% l-alanine			
15% DSCG	Right	<3	32.8° → 19.8°
23.4% trans-4-hydroxy-l-proline			Blue → Yellow

^a As measured from the fingerprint patterns.

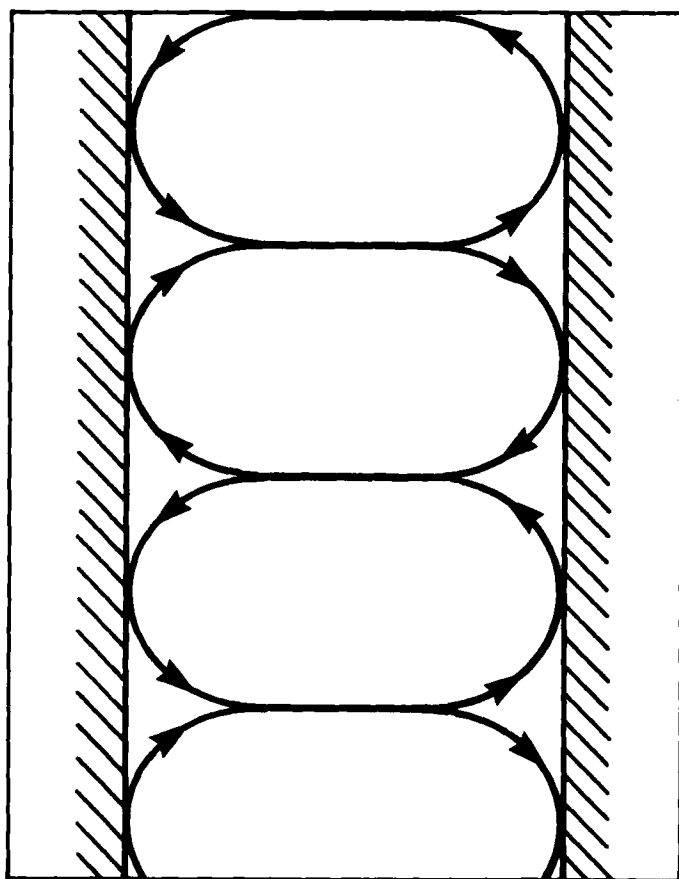


(a)



(b)

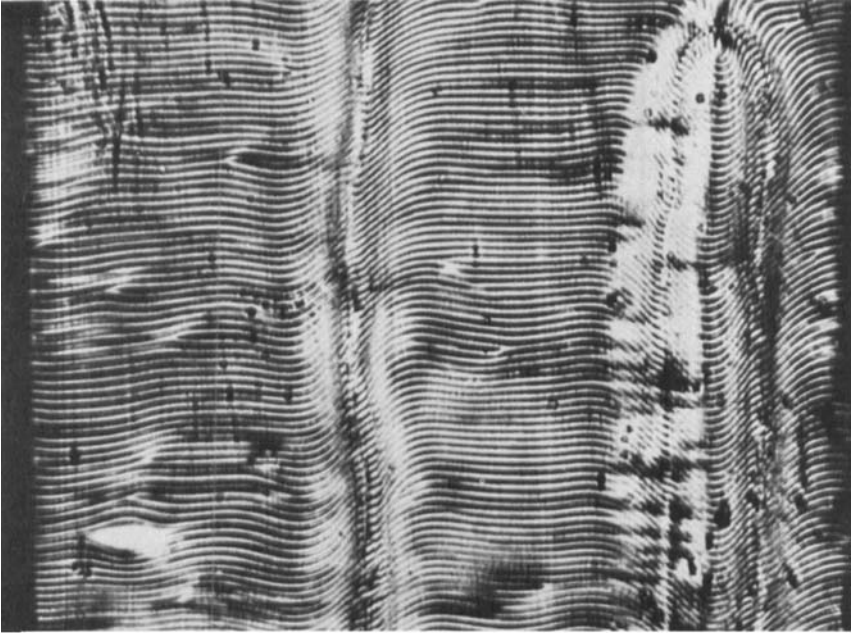
FIGURE 7 See caption after 7(c).



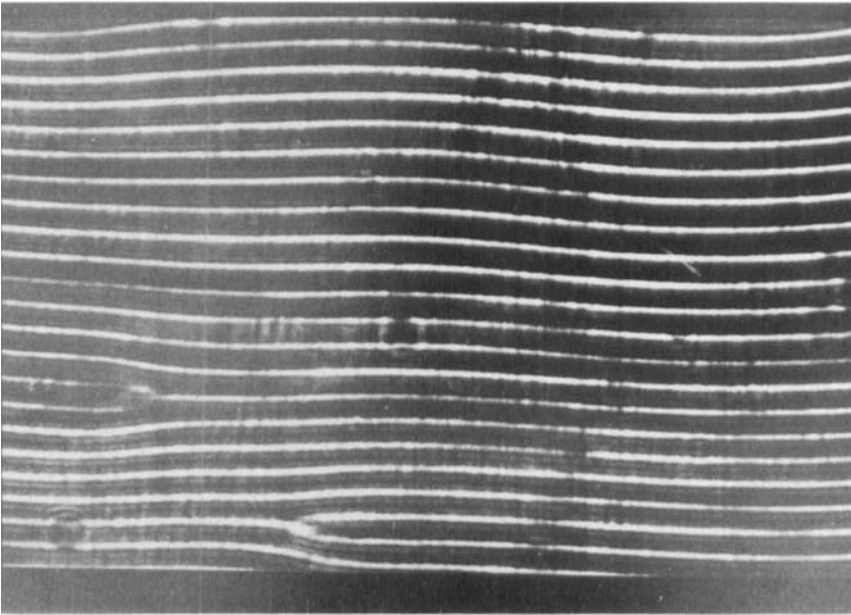
(c)

FIGURE 7 Sample consisting of 17% DSCG, 11% l-proline in water aligned in a 19 kG magnetic field for 5 hours at 20°C. Sample pitch = 20 μm in a capillary of 100 μm thickness. (a) applied magnetic field direction along y direction (magnification $\times 125$); (b) applied magnetic field direction along x direction (magnification $\times 125$); (c) schematic figure of flow pattern of liquid crystal in a capillary.

In a 19 kG H field (Figure 7) the distance between flow lines is $\sim 375 \mu\text{m}$ and increases with decreasing magnetic field, being $\sim 400 \mu\text{m}$ at 15 kG. In a 60 kG field, the distance (in a similar sample) is $\sim 180 \mu\text{m}$ (Figure 8a). Details of the fingerprint region are shown in Figure 8b. After 2 hours in a 60 kG field, the fingerprint periodic texture is well established. After removal from the field, the sample orientation slowly reverts to plane textured cholesteric at rates which depend in a complex way on the wall treatment, the thickness of the sample, and its viscosity. A typical "mixed texture", which then remains stable for weeks, is shown in Figure 8c.



(a)



(b)

FIGURE 8 See caption after 8(c).



(c)

FIGURE 8 Sample consisting of 10.3% DSCG, 3.3% l-alanine, 2.4% Na-d-mandelate in water aligned in a 60 kG magnetic field along x direction for 5 hours at 21°. Sample pitch = 21 μm in a capillary of 300 μm thickness. (a) immediately after removing from field. Distance between flow lines $\sim 180 \mu\text{m}$. (b) 5 fold enlargement of fingerprint region of same sample. (c) same sample, magnification as in (a) after 1 hour out of magnetic field. This pattern remains for weeks.

The pitch of the cholesteric array showed an interesting time dependence in the magnetic field. Pitch *decreased* with time in a 15 kG field (Figure 9), reaching a saturation value after ~ 16 hours. All pitch values reported in this paper were measured after at least 20 hours in the field. The reason for this pitch shortening is not obvious. Since the system is a cholesteric where $\Delta\chi < 0$, the helix axis is \parallel to H , and no helix unwinding or tightening should occur. Considering the aggregates to be cylindrical in shape, then, each cylinder (or hollow square column of the Lydon⁹ model) is, on the average \perp to H . Any chiral interaction *within* the cylinder might then undergo a field induced distortion, with a concomitant effect on the overall chirality of the helix of cylinders. This interesting possibility is being explored in our current work.

VII CONCLUSION

DSCG-H₂O—with or without chiral additives—is an easy-to-prepare lyotropic system of relatively low viscosity which orients in a magnetic field. The nematic system is of Type II, $\Delta\chi < 0$, and the cholesteric system therefore

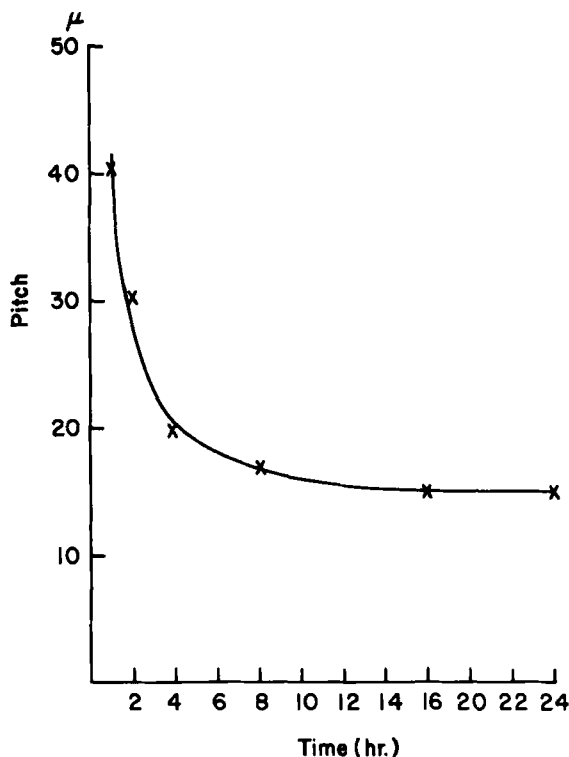


FIGURE 9 Pitch vs time for 8% l-proline in 13% DSCG/water in 15 kG magnetic field at 20°C.

aligns with its helix axis \parallel to H . The constituent element of both nematic and cholesteric phases is probably a cylindrical aggregate, which may have the shape recently suggested by Lydon.⁹ A rich array of defect patterns of hydrodynamic origin develop in both nematic and cholesteric phases.

The nematic phase transition temperatures are very sensitive to the nature of the cation and its concentration, whereas pH has little effect. The pitch of the cholesteric phase can be varied from the visible to the infrared region, and characteristic iridescent colors can be seen in systems doped with amino acids.

Since these systems are aqueous phases with capability of dissolving large concentrations of polar organic molecules, one may anticipate a wide range of solute-solvent interactions allowing study of solute ordering. Their relatively low viscosities allow facile coupling to external torques such as magnetic fields and shear flow.

This work was supported by the National Science Foundation under Grants No. DMR77-07811 and DMR81-07142. The facilities and support of

The Weizmann Institute of Science, which granted a Meyerhoff Fellowship to one of us (MML) for March–July 1981, is also gratefully acknowledged.

References

1. K. Radley and L. W. Reeves, *Can. J. Chem.*, **53**, 2998 (1975).
2. K. Radley, L. W. Reeves and A. S. Tracey, *J. Phys. Chem.*, **80**, 174 (1976).
3. D. M. Chan, F. Y. Fujiwara and L. W. Reeves, *Can. J. Chem.*, **55**, 2396 (1977).
4. F. Y. Fujiwara and L. W. Reeves, *Can. J. Chem.*, **56**, 2178 (1978).
5. L. J. Yu and A. Saupe, *J. Am. Chem. Soc.*, **102**, 4879 (1980).
6. K. D. Lawson and T. J. Flautt, *J. Am. Chem. Soc.*, **89**, 5490 (1967).
7. M. Acimis and L. W. Reeves, *Can. J. Chem.*, **58**, 1533 (1980).
8. N. H. Hartshorne and G. D. Woodard, *Mol. Cryst. Liq. Cryst.*, **23**, 343 (1973).
9. J. E. Lydon, *Mol. Cryst. Liq. Cryst. Lett.*, **64**, 19 (1980).
10. N. H. Hartshorne and G. D. Woodard, *Mol. Cryst. Liq. Cryst. Lett.*, **64**, 153 (1981).
11. K. Radley and A. Saupe, *Mol. Cryst. Liq. Cryst.*, **44**, 227 (1978).
12. P. Diehl and A. S. Tracey, *Can. J. Chem.*, **53**, 2755 (1975).
13. J. Charvolin and Y. Hendrikx, in "Liquid Crystals of One- and Two-Dimensional Order," Ed. by W. Helfrich and G. Heppke, Springer-Verlag, Berlin (1980), p. 265.
14. J. Charvolin, A. M. Levelut and E. T. Samulski, *J. de Phys. Lett.*, **40**, L-587 (1979).
15. C. S. Bak and M. M. Labes, *J. Chem. Phys.*, **62**, 3066 (1975).
16. J. Adams and W. Haas, *Mol. Cryst. Liq. Cryst.*, **30**, 1 (1975).
17. E. Guyon, R. Meyer and J. Salan, *Mol. Cryst. Liq. Cryst.*, **54**, 261 (1979).
18. J. Charvolin and Y. Hendrikx, *J. Physique-Lettres*, **4**, L597 (1980).